Electronic Supplementary Material (ESI) for Environmental Science: Nano.

Supporting information: Transformation of cerium dioxide nanoparticles during sewage sludge incineration

Alexander Gogos[a], Jonas Wielinski[a,b], Andreas Voegelin[a], Hermann Emerich[c] and Ralf Kaegi[a],*

[a] Eawag, Swiss Federal Institute of Aquatic Science and Technology, Überlandstrasse 133, 8600 Dübendorf, Switzerland.

[b] ETH Zürich, Institute of Environmental Engineering, 8093 Zürich, Switzerland

[c] European Synchrotron Facility (ESRF), 71, av. des Martys, 38000 Grenoble, France

* Corresponding author. Tel.: +41 (0)58 765 52 73; e-mail: ralf.kaegi@eawag.ch.

Description of the bubbling bed type pilot scale fluidized bed reactor (FBR)

Reproduced from Wielinski et al.[1]:

The bubbling bed type pilot FBR consists of an incineration unit (heater, reactor, sludge feed) and an off gas unit (heat exchanger, two electrostatic precipitators (ESPs), ash bin). A mass flow controller (red-y, Voegtlin, Switzerland) was used to adjust the gas flow between 50 and $200\ L_n/min$. The incoming air was heated by a 15 kW electric resistance heater (LE 10000 DF-R HT, Leister, Switzerland) and passed the windbox and a distributor plate (d = 10 cm) with 120 evenly distributed holes (d = 1 mm). The pressure in the windbox beneath the distributor plate was approximately 1.45 kPa above atmospheric pressure. The sand bed (h = 5 cm, w = 0.7 kg, 630 > d_{sand} > 800 µm) above the distributor plate was fluidized at bubbling bed type conventional fluidization conditions [2, 3]. The bed was composed of Geldart group B solids [4, 5] with a theoretical minimal fluidization occurring at a 0.9 kPa pressure drop [2]. Typical operation conditions were $T_{sand\ bed} \approx 820 - 840\ °C$ and air flow $\approx 120\ L_n/min$ leading to a fluidization with a dimensionless gas velocity $u^* = 0.38$ and a dimensionless particle diameter $d^* = 11.75$ (conventional fluidization conditions) [2]. Under typical bed loadings the pressure above the sand bed was approximately 0.35 kPa above atmospheric pressure, thus a pressure drop of 1.1 kPa occurs. Dried sludge was continuously fed via a spiral conveyor at rates of 0.8 kg/h. The reactor (or freeboard) temperature fluctuated between 400 and 800 °C, depending on the sludge load in the fluidized bed. The reactor pressure was held constant at -1.6 kPa by a draught fan at the end of the off gas unit. A lambda sensor monitored residual oxygen concentrations and CO equivalents (COe) at the upper end of the reactor column. Residual oxygen concentration depended on the fuel load in the bed and typically varied between 12% and 16%. COe was usually below 100 ppm, depending on the temperature in the sand bed and reactor. Higher temperatures in the sand bed and the reactor lead to lower values of COe. A heat exchanger, installed at the upper end of the reactor reduced the off gas temperature to 110 °C. The off gas was further fed into the first of two identical electrostatic precipitators (ESPs) (OekoTube-Inside, Oekosolve, Switzerland). A flexible resistance heater was wrapped around each ESP to keep the temperature above the dew point. Particles passing the ESP units were collected in a filter bag (FB) at the end of the off gas stream. After an experiment, the ESP units were agitated and the particles collected from the ash bin.

Tables

Table S1: Primary particle and agglomerate/aggregate sizes of the different CeO_2 particles used in this study.

	Primary particle size (TEM) [nm][1]			Particle size in spiking dispersion (LS) [µm][2]			Particle size in spiking dispersion (TEM) [nm][3]	
	Median	Mean	StdDev	Median	Mean	StdDev	Min. Feret	StdDev
CeO_2-s1	4.2	4.3	1.2	<<0.4	<<0.4	n.a.	10.8	4.2
CeO_2-s2	23.7	26.2	11.5	2.4	2.9	2.3	342	685
CeO_2-s3	n.a.	n.a.	n.a.	16.5	356	510	n.a.	n.a.

[1]The primary particle size of CeO_2-s1 was determined from 91 measurements, that of CeO_2-s2 from 30 measurements.
[2]The particle size in the spiking dispersion was determined by laser diffraction analyses (Beckman Coulter LS 13 320). The particle size for CeO_2-s1 was below the lower size limit of the instrument (0.4 µm).
[3]The particle size in the spiking dispersion was additionally determined using particle sizer plugin in ImageJ[6] on HAADF images. 537 aggregates were analyzed for CeO_2-s1 and 55 for CeO_2-s2.
n.a.: not available

Table S2: Mass balance of all experiments. SLG represents sludge, FA fly ash, BA bottom ash and FB filterbag. m is the absolute mass in g, c is the concentration in µg g^{-1}. Concentrations represent the average values from three replicate measurements. The ash content of the sludge was determined by combusting 100 mg of sample in a muffle oven. The oven was heated to 900°C at a heating rate of 10 K min^{-1} and then kept at that temperature for 1 h. For total carbon (TC) determination, 1-15 mg of sample (depending on the expected carbon content) were weighed into tin capsules, amended with vanadium oxide catalyst and determined using a Euro EA CHNSO Elemental analyzer (HEKAtech GmbH, Germany). The system was calibrated using Acetanilide and a reference soil was measured additionally for quality assurance. The burn-off in the FA was calculated as $\%burn-off\ FA = 100 - \left(\frac{\%TC\ FA}{\%TC\ SLG} \cdot 100\right)$. Ash recovery ($rc\%_{ash}$) was calculated as $rc\%_{ash} = \frac{(m_{FA} \cdot (1 - f_{TC(FA)})) + (m_{BA} \cdot (1 - f_{TC(BA)})) + (m_{FB} \cdot (1 - f_{TC(FA)}))}{m_{SLG} \cdot f_{ash}} \cdot 100$. Mass recovery of Ce over the whole experiment ($rc\%_{Ce}$) is scaled to the recovery of the ash content and calculated as $rc\%_{Ce} = \left(\frac{\left(m_{FA} * c_{FA}^{Ce}\right) + \left(m_{BA} * c_{BA}^{Ce}\right) + (m_{FB} * c_{FB}^{Ce})}{m_{SLG} * c_{SLG}^{Ce}} \cdot 100\right) \cdot \frac{1}{rc\%_{ash}} \cdot 100$. An effective enrichment factor (EF_{eff}) for Ce was calculated for the ash as $EF_{eff} = \frac{c_{ash}^{Ce}}{c_{SLG}^{Ce}} = \frac{1}{c_{SLG}^{Ce}} \cdot \frac{(m_{FA} * c_{FA}) + (m_{BA} * c_{BA}) + (m_{FB} * c_{FB})}{m_{FA} + m_{BA} + m_{FB}}$. Expected enrichment factors (EF_{exp}) assuming exclusive accumulation of Ce in the ash corresponding to the mass ratio of sludge to the ash were calculated as follows: $EF_{exp} = \frac{m_{SLG}}{m_{FA} + m_{BA} + m_{FB}}$.

Sample	m SLG [g]	m FA [g]	m BA [g]	m FB [g]	c SLG [µg/g]	c FA [µg/g]	c BA [µg/g]	c FB [µg/g]	c_{ash} %	%TC SLG	%TC BA	% TC FA	% burn-off in FA	$rc\%_{ash}$	$rc\%_{Ce}$	EF_{eff}	EF_{exp}
CeO_2-s1	380.00	7.58	122.00	7.82	1033.89	2421.53	2865.62	1831.87	34.1	30.22	0.07	5.85	80.63	105.27	92.43	2.69	2.77
CeO_2-s2	215.92	7.47	75.09	0.88	2290.83	3115.33	5629.70	2487.40	33.0	29.41	0.12	2.68	90.90	116.66	77.67	2.34	2.59
CeO_2-s3	226.26	13.66	77.68	5.51	1184.73	1895.57	3188.27	165.14	33.7	29.26	0.13	2.10	92.83	126.36	81.03	2.39	2.34
N1	500.00	5.21	154.44	5.06	93.24	438.92	216.55	502.74	30.4	37.36	0.11	2.56	93.15	108.08	75.96	2.49	3.04

N2	1000.00	51.00	275.00	1.08	9.79	31.54	19.85	20.94	31.9	26.36	n.d.	2.22	91.58	102.17	70.91	2.22	3.06

Table S3: Recovery of spiked CeO_2.

	Ce added [mg]	m_{total} SLG [kg]	c_{exp}SLG [mg/kg]	c SLG [mg/kg]	Spike recovery %
CeO_2-s1	552.00	0.47	1174.47	1033.89	88.03
CeO_2-s2	722.80	0.25	2891.2	2290.83	79.23
CeO_2-s3	722.80	0.25	2891.2	1184.73	40.97

Table S4: Results of the LCF analyses to Ce K- and L_{III}-edge XANES spectra.

					Nano-CeO_2		Bulk-CeO_2		Ce(III)PO_4		Ce-allanite	
Data	**rfactor**	**chinu**	**chisqr**	**sum**	**weight**	**error**	**weight**	**error**	**weight**	**error**	**weight**	**error**
K-edge XANES												
SLG CeO_2-s1	1.77E-05	2.60E-06	4.60E-04	1.00	0.50	0.02	0.10	0.02	0.09	0.01	0.30	0.01
FA CeO_2-s1	1.91E-05	2.70E-06	4.70E-04		0.060	0.002			0.250	0.012	0.690	0.013
L_{III} edge XANES												
SLG CeO_2-s2	5.47E-04	1.22E-04	2.67E-02	0.986			0.986	0.019				
FA CeO_2-s2	4.54E-04	9.73E-05	2.13E-02	0.99			0.674	0.001			0.316	0.001
SLG CeO_2-s3	8.51E-04	1.94E-04	4.25E-02	0.990			0.990	0.025				
FA CeO_2-s3	2.99E-03	7.05E-04	1.54E-01	1.017			0.728	0.004			0.289	0.004
SLG N1	6.25E-03	1.55E-03	3.40E-01	1.029			0.682	0.006			0.347	0.005
FA N1	4.28E-03	1.32E-03	2.90E-01	1			0.220	0.005			0.780	0.005
SLG N2	4.38E-02	1.36E-02	2.97E+00	1.078			0.603	0.017			0.474	0.016
FA N2 pilot	4.22E-02	1.04E-02	2.27E+00	0.925	0.300	0.016					0.625	0.014
FA N2 fullscale	3.27E-02	9.99E-03	2.19E+00	1.028			0.344	0.015			0.683	0.013

Figures

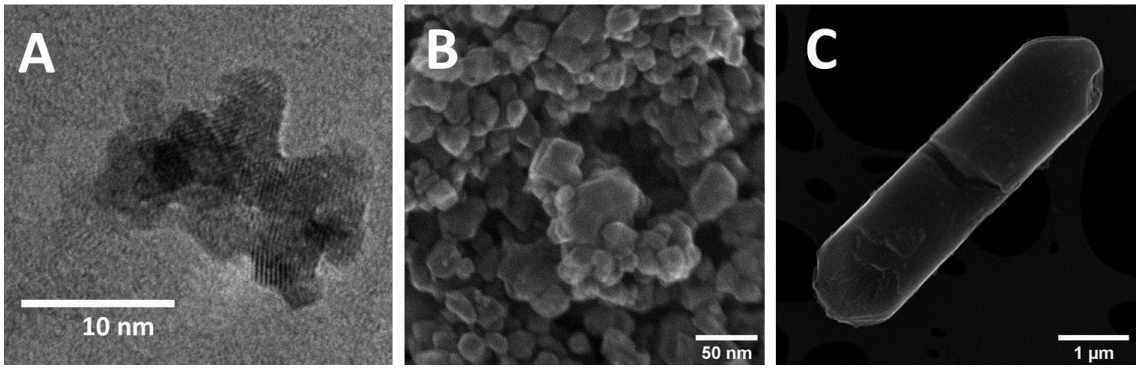

Fig. S1: (A) TEM-bright field image of the CeO_2-s1 particles. (B + C) STEM-secondary electron images of the CeO_2-s2 and CeO_2-s3 particles, respectively.

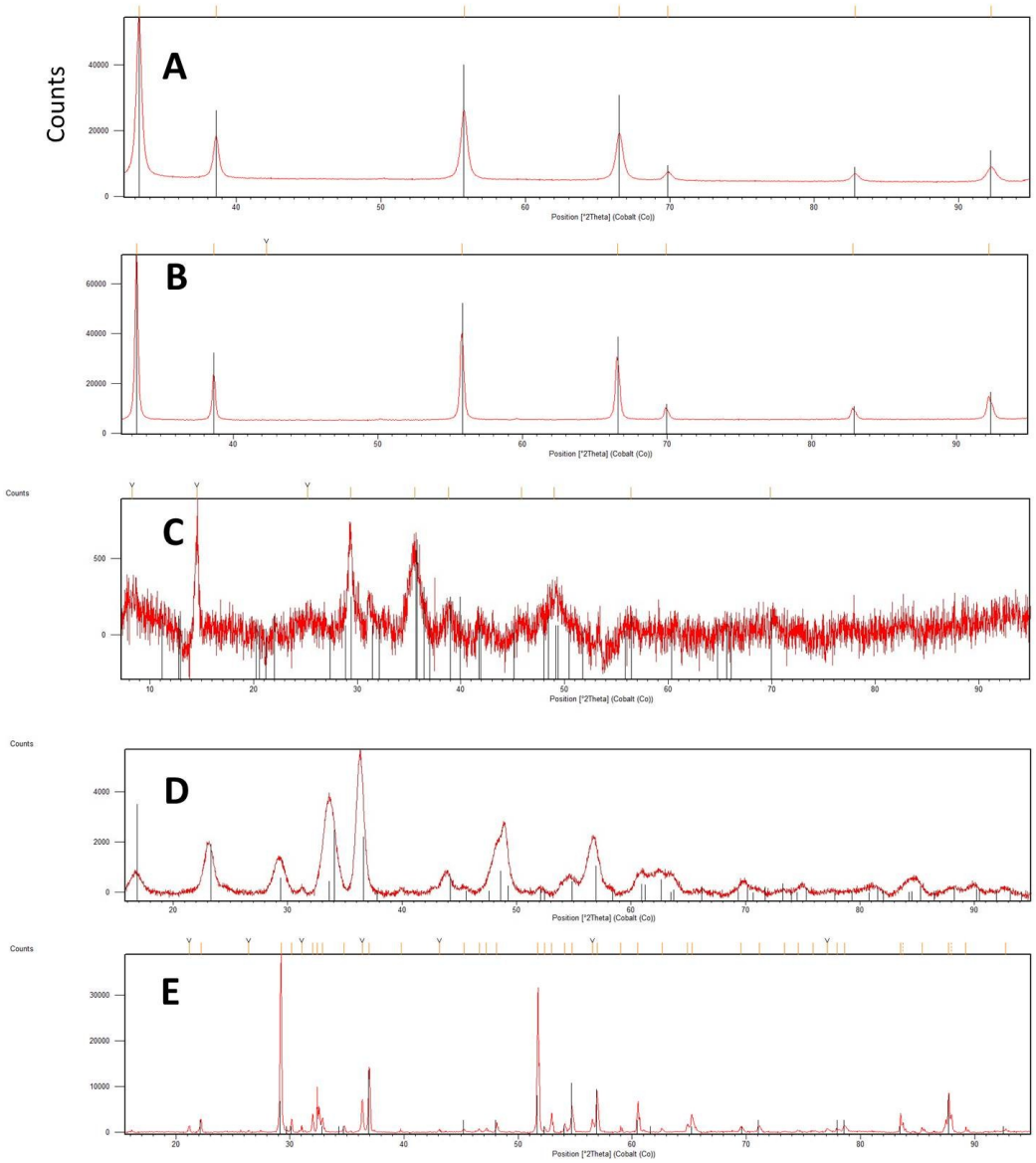

Fig. S2: Powder X-ray diffraction spectra of (A) CeO_2-s2, (B) CeO_2-s3 (C) Ce-allanite, (D) rhabdophane ($CePO_4$) and (E) Ce-parisite. Black lines indicate characteristic peaks for the respective structure.

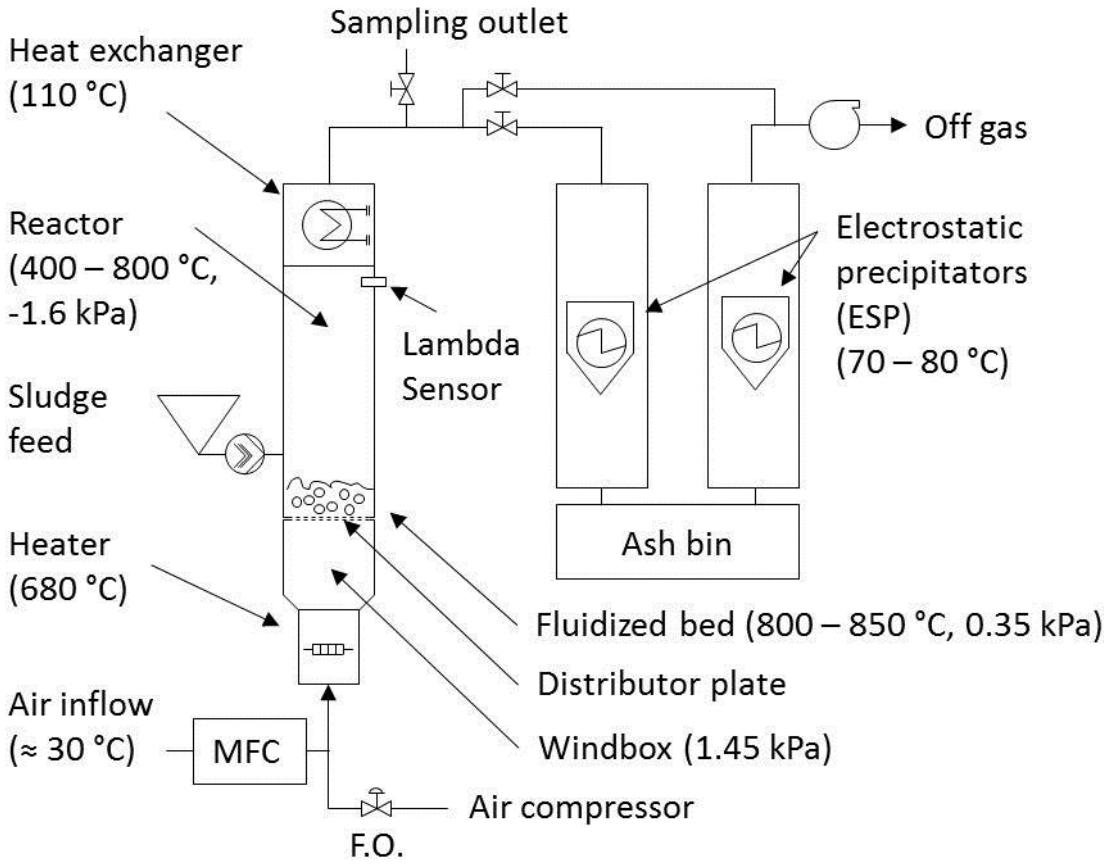

Fig. S3: Schematic of the pilot fluidized bed reactor used for the incineration experiments. MFC: mass flow controller. Reproduced from Wielinski et al.[1].

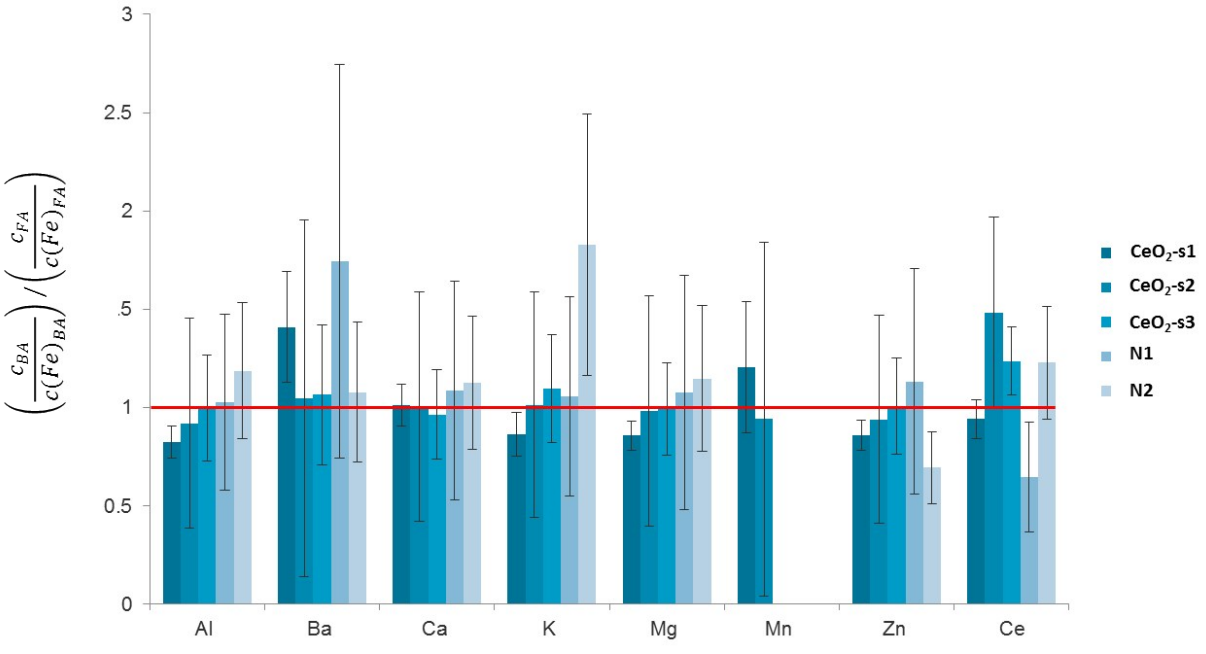

Fig. S4: BA:FA ratios $\left(\frac{c_{BA}}{c_{BA}^{Fe}}\right)/\left(\frac{c_{FA}}{c_{FA}^{Fe}}\right)$ obtained from Fe-normalized concentrations for different elements. The error bars show the error of the ratio obtained from error propagation according to $\frac{\Delta r}{r} = \left(\frac{\Delta c}{c} + \frac{\Delta cFE}{cFE}\right)_{BA} + \left(\frac{\Delta c}{c} + \frac{\Delta cFE}{cFE}\right)_{FA}$, where r is the BA:FA ratio, c is the concentration of the element of interest and cFE the iron concentration in the respective ash fraction. Elemental concentrations were determined using inductively coupled plasma (ICP) optical emission spectrometry except for Ce, which was determined using ICP mass spectrometry. The same digests were used for both analyses. Recoveries for the different elements were between 79% (Ca) and 102% (Al) for NIST SRM 2782 Industrial sludge.

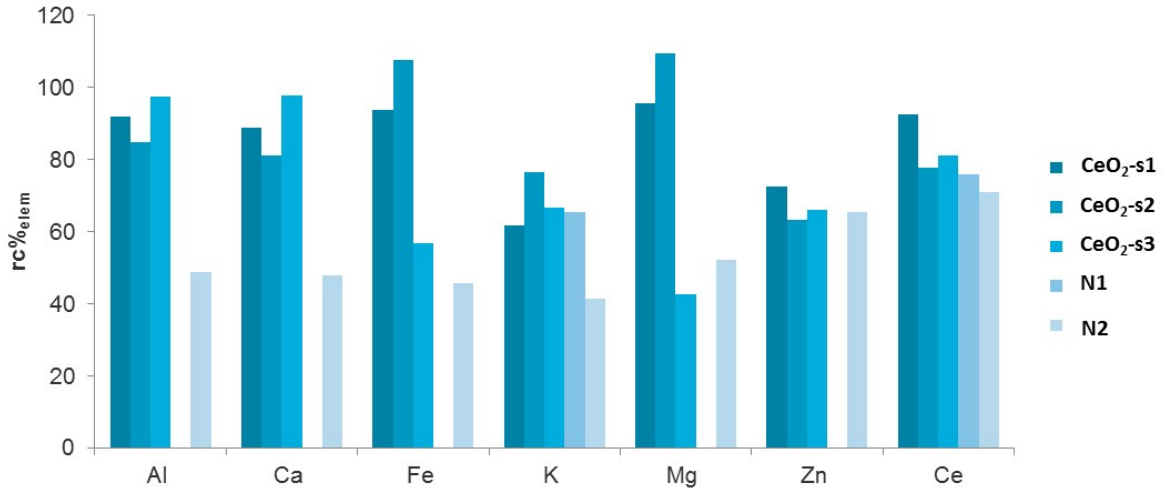

Fig. S5: Recovery of selected elements over the whole experiment scaled to the ash recovery, calculated after eq. 2 in the main text.

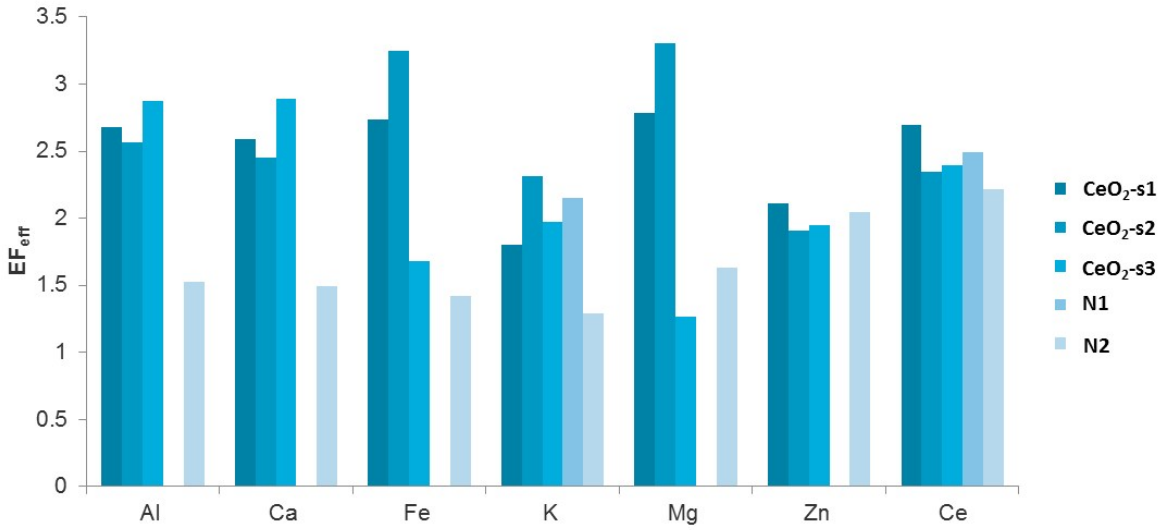

Fig. S6: Effective enrichment factors (EF_{eff}) for selected elements, calculated after eq.3 in the main text.

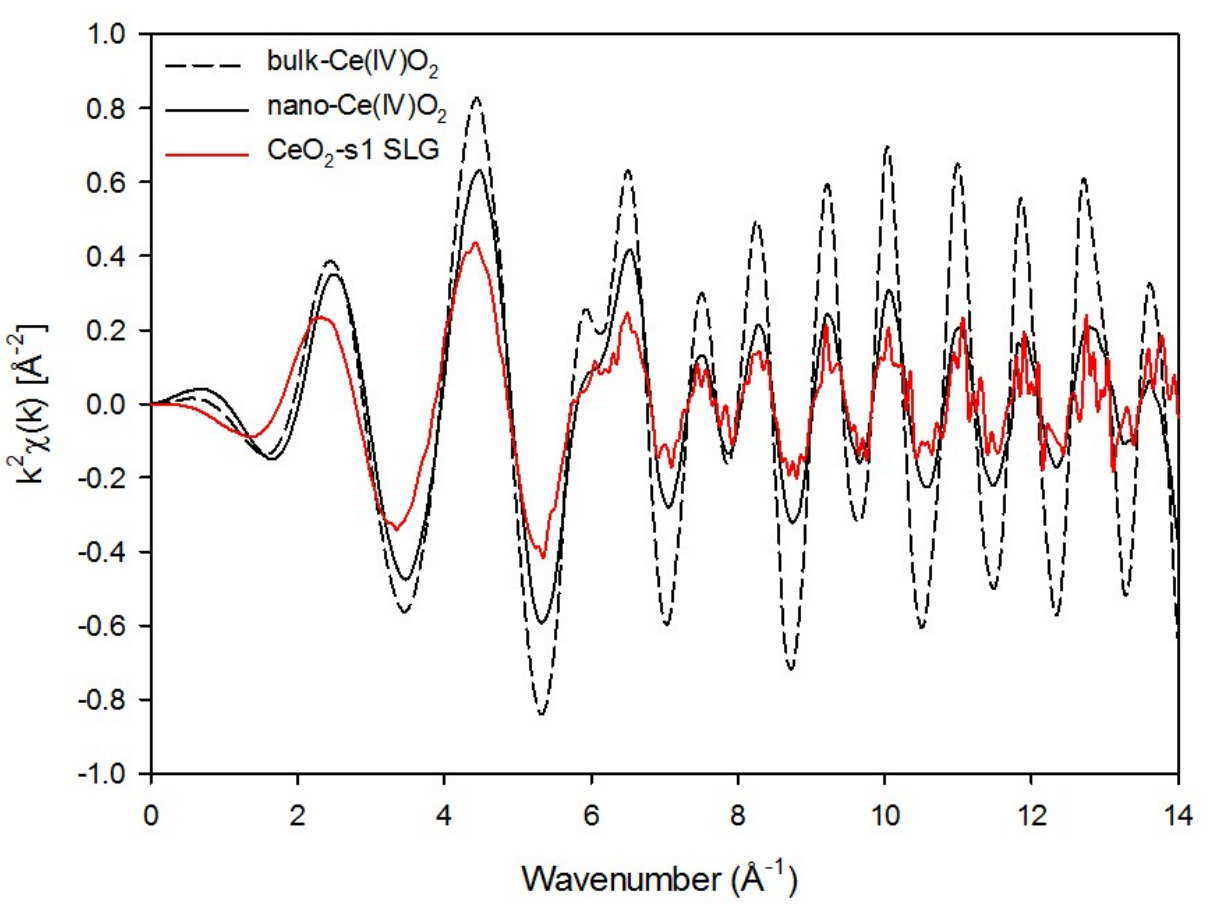

Fig. S7: k^2-weighted EXAFS obtained from Ce K-edge data of the nano- (solid black line) and bulk Ce(IV)O_2 reference (dashed black line) as well as CeO_2-s1 SLG (red line).

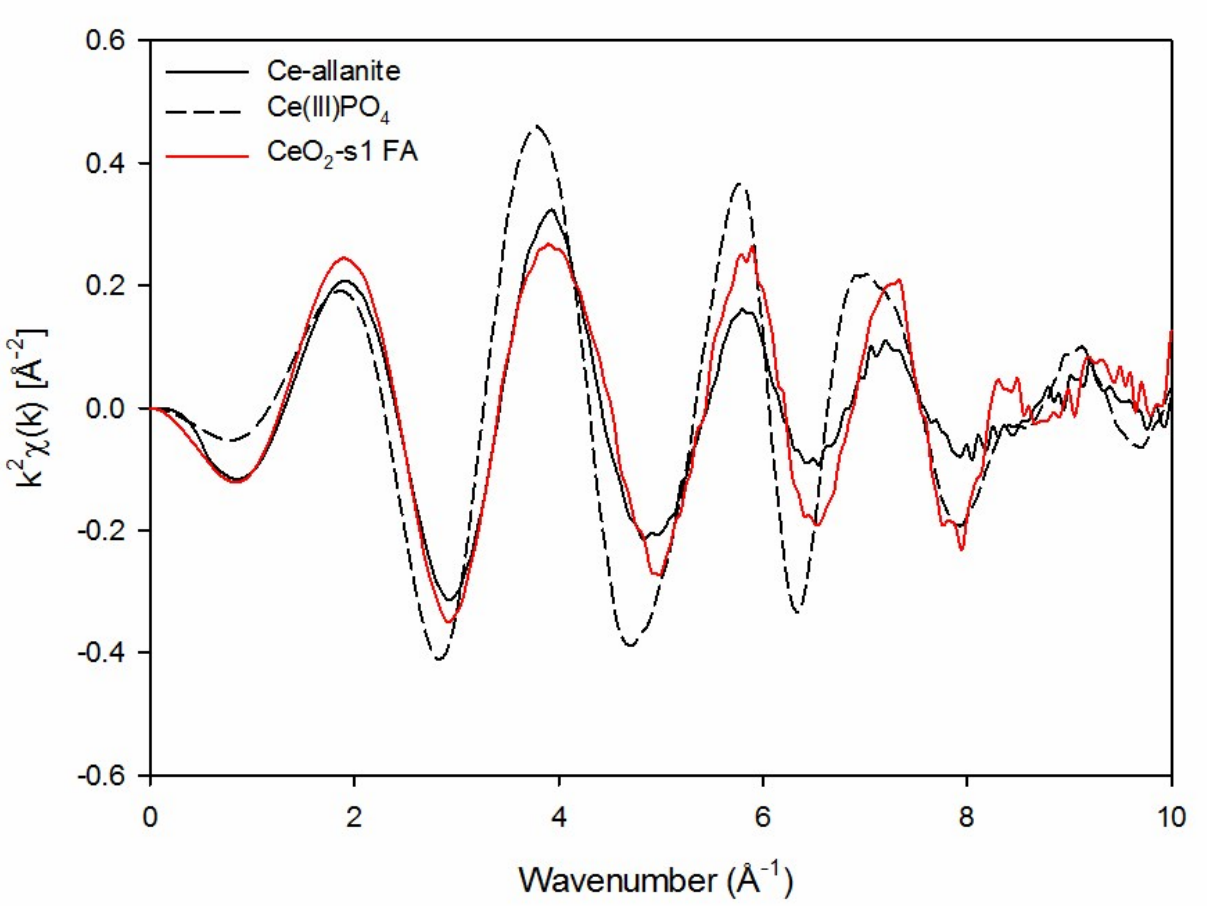

Fig. S8: k^2 weighted EXAFS obtained from Ce K-edge data of the Ce-allanite (solid black line) and Ce(III)PO_4 reference (dashed black line) as well as the CeO_2-s1 FA (red line).

A

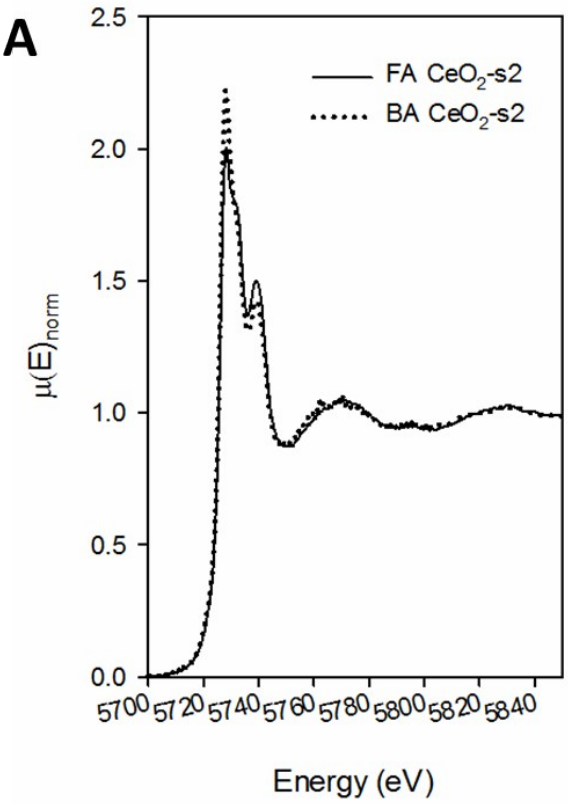

B

	Data	FA CeO2-s2	BA CeO2-s2
	rfactor	4.54E-04	8.02E-04
	chinu	9.73E-05	1.75E-04
	chisqr	2.13E-02	3.83E-02
	sum	0.99	0.988
nano-CeO2	weight		
	error		
bulk-CeO2	weight	0.674	0.586
	error	0.001	0.002
Ce(III)PO4	weight		
	error		
Ce-allanite	weight	0.316	0.402
	error	0.001	0.002

Fig. S9: (A) Comparison of Ce L_{III}-edge XANES spectra obtained from the CeO_2-s2 FA (solid line) and BA (dotted line) and (B) corresponding LCF results.

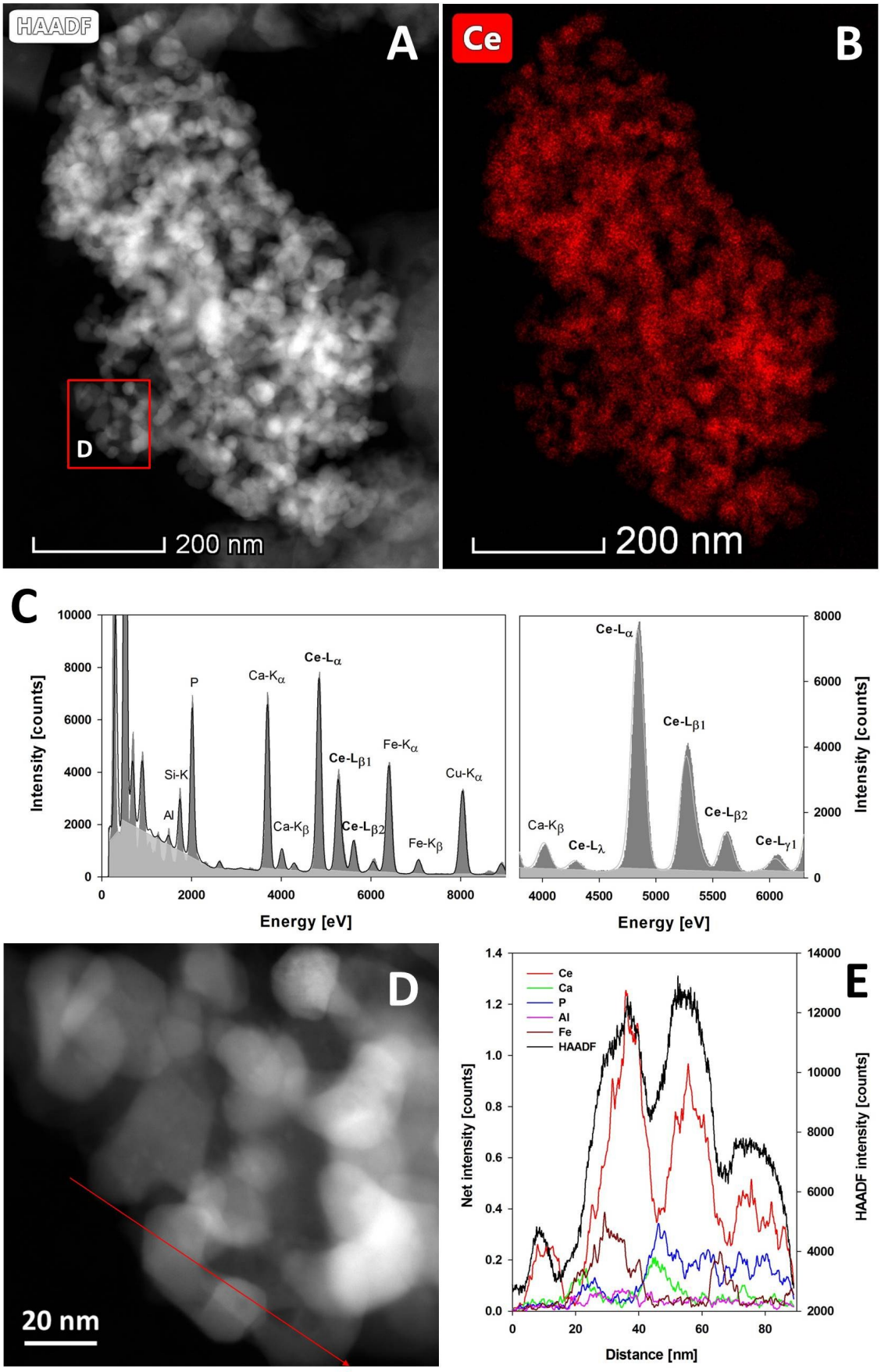

Figure S10 (A) STEM-HAADF micrograph and (B) the corresponding Ce distribution map of a Ce-agglomerate observed in the CeO_2-s1 FA sample. Cerium distribution in B is shown in red. (C) EDX spectrum integrated over the whole image shown in (A).

In addition to the raw EDX spectrum (dark grey) also the calculated background (light gray overlay) and the modelled EDX peaks (black line) are shown for clarity. (D) is a magnification of the area highlighted in (A). The red arrow in (D) shows the direction of the line scan shown in (E). Signal intensities (counts) over along the line scan are shown for Ce (red), Fe (brown), Ca (green), Al (violet), and P (blue).

References

1. J. Wielinski, A. Gogos, A. Voegelin, C. Mueller, E. Morgenroth and R. Kaegi, Transformation of Cu and Zn - (nanoparticles) during the incineration of digested sewage sludge (biosolids), *Submitted Apr 02 2019 to Environ. Sci. Technol.*, 2019.
2. H. A. Jakobsen, in *Chemical Reactor Modeling*, Springer, Berlin, Heidelberg, 2009.
3. J. G. Yates and P. Lettieri, in *Fluidized-Bed Reactors: Processes and Operating Conditions*, Springer International Publishing, Cham, 2016, DOI: 10.1007/978-3-319-39593-7_4, pp. 111-135.
4. L. Hagesaether, H. A. Jakobsen and H. F. Svendsen, Theoretical analysis of fluid particle collisions in turbulent flow, *Chem. Eng. Sci.*, 1999, **54**, 4749-4755.
5. L. Hagesaether, H. A. Jakobsen and H. F. Svendsen, Modeling of the Dispersed-Phase Size Distribution in Bubble Columns, *Industrial & Engineering Chemistry Research*, 2002, **41**, 2560-2570.
6. T. Wagner, ij-particlesizer: v1.0.9 Snapshot release (Version v1.0.9-SNAPSHOT).*Journal*, 2017, DOI: http://doi.org/10.5281/zenodo.820296.